REAL-TIME MONITORING OF FLUORESCENCE ANISOTROPY AND TEMPERATURE DURING PROCESSING OF BIAXIALLY STRETCHED POLYPROPYLENE FILM

Anthony J. Bur and Steven C. Roth
Polymers Division
National Institute of Standards and Technology
Gaithersburg, MD 20899-8542

Abstract

Using an optical sensor, fluorescence anisotropy and fluorescence temperature measurements were carried out during the processing of biaxially stretched polypropylene films in a tenter. The fluorescence derived from a dye that was doped into the resin. Anisotropy measurements were made as a function of machine stretching ratios.

Introduction

Continuous processing of biaxially oriented polypropylene (BOPP) films involves stretching in a tenter frame at elevated temperatures. The properties and performance of the film are determined by the molecular orientation that is created in the film by applied extensional stresses. Machine parameters that can be adjusted to control molecular orientation are stretch ratios, strain rates, and temperature.

Laboratory methods to characterize molecular orientation of the film product, such as X-ray diffraction and birefringence, can only be used in post-processing tests. Moreover, they exclusively reflect or are dominated by crystalline orientation. A method for on-line continuous monitoring of molecular orientation is desirable because it can yield a database record of the process, can be utilized immediately to adjust machine parameters to make a desired product, and can be used as a sentry to detect quality problems. This method should primarily reflect amorphous orientation, which has a more profound effect on the marginal improvement or variation of film properties.

To these ends, we report the development and implementation of an on-line, real-time sensor based on fluorescence spectroscopy to monitor both orientation and temperature of biaxially stretched polypropylene. This sensor combines two process monitoring concepts, temperature and orientation, that we have pursued using fluorescence techniques during the past several years.[1,2] The measurement relies on the presence of a fluorescent dye that is mixed with the resin at low concentrations, less than 10^{-5} mass fraction of dye in the resin. The dye used for this work is bis (di-tert butylphenyl) perylenedicarboximide (BTBP), a dye molecule that possesses large geometrical anisotropy and belongs to a class of dyes that show marked temperature dependence in the shape of their fluorescence spectrum. The large geometrical anisotropy enhances its orientation in extensional flows. Its size precludes inclusion in the crystalline structure of PP. The molecular structure of BTBP is shown in Fig. 1, where the double headed arrow is the direction of the absorption dipole.

Fluorescence anisotropy measurements yield information about the orientation of the absorption dipole moment of a fluorescent dye that has been interrogated with polarized light.(1,2) For this application, the direction of the incident light is polarized alternately in the machine direction (MD) and the transverse direction (TD). Orientation information is obtained from the polarization of the emitted fluorescent light. We measure two anisotropies, r_M and r_T, corresponding to excitation light polarized in the machine and transverse directions:

$$r_M = \frac{I_{MM} - I_{MT}}{I_{MM} + 2I_{MT}} \qquad r_T = \frac{I_{TT} - I_{TM}}{I_{TT} + 2I_{TM}} \qquad (1)$$

where I_{MM} and I_{MT} are respectively the intensities of fluorescent light polarized in the machine and transverse directions, produced by incident light polarized in the machine direction, and I_{TT} and I_{TM} are respectively the intensities of fluorescent light polarized in the transverse and machine directions, produced by incident light polarized in the transverse direction. Molecular models have been developed to relate r_M and r_T to orientation factors describing the orientation distribution of the dye's absorption dipole moment.[3] In this paper, we will not discuss molecular orientation factors, but will confine our attention to sensor development and to on-line measurements of r_M and r_T. Eq. (1) expresses anisotropy as the difference between intensities of mutually perpendicular polarizations of fluorescence divided by the approximate total fluorescence intensity. r is a dimensionless quantity, theoretically limited to the range -0.5 to +1 and independent of the amount of dye.

The second function of the sensor, to monitor temperature, is based on the shape of the fluorescence spectrum and its dependence on temperature. The technique has been described in detail in a previous publication.[1] Briefly, plotting the ratio of intensities at two wavelengths vs.

temperature forms a calibration curve. Consider the spectra of BTBP doped into polypropylene in Fig. 2. Here, spectra for BTBP excited at 488 nm are plotted for a series of temperatures from 132 °C to 196 °C. The trough between the two peaks at 528 nm and 563 nm becomes shallower as temperature increases. The ratio of peak to trough intensity,

$$\theta = I_{563} / I_{548} \qquad (2)$$

is a nearly linear function of temperature, as will be seen, and independent of the amount of dye.

Experimental Apparatus and Procedure

Sensor design is shown in Fig. 3 & 4 and is described in more detail in [2]. The sensor is a 6 x 3.8 x 5 cm block of stainless steel into which three channels have been machined. Two channels are used for the anisotropy measurement. Each contains a bundle of thirteen optical fibers. One fiber transmits excitation light from a 488 nm argon ion laser to the film. The twelve remaining fibers collect fluorescence from the film and send it to the photomultiplier (PMT) detectors.

As shown in Fig. 4, a beamsplitter divides the excitation light from the laser into two beams directed to optical fibers in the center and side channels. Shutters open these channels one at a time. Light polarized in the **machine** direction is produced when light travels along the center channel path and directly through the calcite crystal. Light polarized in the **transverse** direction is produced by light that travels the side channel path, reflects off the mirror, enters the calcite crystal from the side, reflects off the diagonal boundary between crystals, and exits through the aperture in the front. The rectangular cross section of the sensor serves as an external reference for the direction of polarization.

In the reverse direction, fluorescence passing directly through the crystal and collected by the center channel fibers is polarized in the machine direction. Fluorescence that is internally reflected at the diagonal boundary between calcite crystals, directed to the mirror, and reflected into the collection fibers in the side channel is polarized in the transverse direction. At the entrance to the PMT detectors, the light passes through a dispersion prism that shunts off stray 488 nm excitation light and through wide-band filters.
In order to account for the difference between fluorescent light transmission through the side and center channels, calibration of the sensor is necessary. This involves obtaining a value for g, the ratio of transmissivities in the two branches. The calibration consists in measuring r_M and r_T of an oriented film at room temperature, then rotating the film 90° and repeating the measurements to obtain r'_M and r'_T. At 0° the expressions for r containing the g-factor are

$$r_M = \frac{I_{MM} - gI_{MT}}{I_{MM} + 2gI_{MT}} \qquad r_T = \frac{gI_{TT} - I_{TM}}{gI_{TT} + 2I_{TM}} \qquad (3)$$

At 90° we have

$$r'_M = \frac{I_{MM} - gI_{MT}}{I_{MM} + 2gI_{MT}} \qquad r'_T = \frac{gI_{TT} - I_{TM}}{gI_{TT} + 2I_{TM}} \qquad (4)$$

The equivalence between the 0° and 90° measurements dictates that

$$r'_M = r_T \qquad r'_T = r_M \qquad (5)$$

These two equations provide two independent values of g, which should equal each other if experimental error is low.

The third channel in the sensor contains collection optical fibers that transmit fluorescence to the PMT detectors for the temperature measurements. This is shown as the dashed line in the sensor body of Fig. 4. These fibers direct the light to a beamsplitter that separates the fluorescence into two beams that are filtered at the trough and peak wavelengths with narrow bandpass filters. The ratio of the trough to peak intensities is then used to calculate the temperature from a calibration curve.

The biaxially stretched film material is made from isotactic polypropylene doped with BTBP dye. BTBP was purchased from Aldrich Chemical Co.[4] Doping of the dye into the polypropylene resin was carried out by pouring a solution of BTBP dye in toluene over resin pellets, followed by evaporation of the solvent, leaving behind pellets coated with BTBP. These pellets and additional neat polymer were then passed through a twin-screw extruder at 200 °C and repelletized. The final concentration of dye in the resin is 6.6 x 10^{-6} mass fraction. Film thickness was 25 μm. Note that concentration uniformity of the die and thickness uniformity of the film are not essential since the r's (Eq. 3) and θ (Eq. 2) are all normalized.

For on-line monitoring, the sensor was mounted in the tenter oven annealing zone 15 mm above the film. Thus, the properties of the film were monitored immediately after TD stretching. The sensor could be placed at any desired TD position by means of a traversing mechanism. For this paper, measurements were taken at the tenter centerline and near the "right" and "left" chain edges.

By means of the same mechanism, the sensor could be raised and shuttled to a background measurement station where anisotropy readings were taken at process temperature against a non-fluorescent, non-reflective black surface. A background measurement series preceded each Right - Center - Left fluorescence measurement sequence. Background intensities I^b_{MM}, I^b_{MT}, I^b_{TT} and I^b_{TM} were obtained and subtracted from the corresponding intensities measured later on oriented film.

Each individual I measurement was a photon count over 1 s. Ten such measurements of I_{MM} and I_{MT} were taken simultaneously, then the shutters were switched to repeat the procedure for I_{TT} and I_{TM}. This sequence was repeated 10 to 20 times in a row, then TD position was changed. The r

data reported below are therefore based on averages of 100 to 200 I values.

The film was stretched sequentially, MD first, followed by TD stretch. The MD and TD mechanical stretch ratios, s_M and s_T, were varied systematically to study the relationship between fluorescence anisotropy and process parameters. All nine combinations of s_M = 4, 5, 6 and s_T = 6.6, 8, 10 were tested. Since winding speed and tenter stretch zone length were kept constant, changes in stretch ratio were accompanied by proportionate changes in strain rate.

Results and Discussion

Fig. 5 shows typical results of the fluorescence temperature measurement along with readings from a thermocouple that was positioned in the air 12 mm away from the film. The process was operating at steady state. Surprisingly good agreement between thermocouple and fluorescence data is observed, allowing for air-film thermal lag.

The fluorescence temperature was calibrated by slowly raising the oven temperature from about 70°C to about 150°C then lowering it back to 70°C with a stationary piece of BOPP film. The ratio θ and air temperature T were measured simultaneously as in the preceding paragraph. The result is seen in Fig. 6. The increasing and decreasing temperature data are very well fitted by distinct straight lines, which differ slightly (3%) in slope. The difference can be entirely explained by the air-film thermal lag. Taking the averages of slopes and intercepts produces an accurate calibration equation.

The g-factor was determined following the procedure above. The relative errors of closure of Eq. 5 are plotted vs. g in Fig. 7. One vanishes at g = 0.318 the other at g = 0.337. This discrepancy is negligible. The root mean square relative error is minimized for g=0.327.

The standard deviation of r can be estimated from the variances and covariances of the I^b_{kl} and I_{kl}'s through a first order Taylor series approximation to r derived from Eq. 3. [5] Note that each I_{kl} in this equation is a *net* intensity, so I_{kl} - I^b_{kl} should be substituted for I_{kl}. The indirect approximate calculation method is necessitated by the fact that I_{kl} and I^b_{kl} values are not paired. For all cases tested, we found std(r_T) between 0.006 and 0.008. std(r_M) was larger, ranging from 0.03 to 0.07. However, even this is not a concern, since the relevant quantity is the standard error of the mean, which is smaller than the standard deviation by a factor √n, where n = number of data values, which was > 100 here.

The data from the nine stretch ratio experiments collected at the Center position are shown in Fig. 8 & 9. In Fig. 8, r_M is plotted against s_M, with s_T as parameter, since intuitively, s_M should be the primary determinant of r_M. Indeed, r_M generally increases with s_M. Less obvious is the fact that r_M also increases to a lesser extent with s_T. This can be attributed to the fact the MD stretch contributes to r_M by reducing out-of-plane molecular orientation prior to the TD stretch.

A multiple regression yields

$$r_M = -0.790 + 0.118\, s_M + 0.0544\, s_T \quad (R^2 = 0.77) \qquad (6)$$

The statistical significance of both coefficients is very high, and potential second or higher-order terms are not significant. The standard error of fit is 0.082. Whether this moderate lack of fit is due to experimental error or to other factors controlling orientation is unknown. However, crystallinity plays no role because the dye is present in the amorphous phase only.

The interpretation of Fig. 9 is more problematic in that r_T does not monotonically increase with s_T or s_M. Part of the difficulty may be due to the smaller range of r_T compared to r_M. This can be seen more clearly in Fig. 10, which includes data from all TD positions. Another important conclusion from this figure is the absence of correlation between r_M and r_T. Hence, these two orientation indices are independent. This is not surprising in a biaxially orientated film, which requires two orientation factors for complete characterization.

In Fig. 10, also note the systematic difference in r_T between the Right, Center and Left positions. In fact, this difference is comparable in magnitude to some of the effects in Fig. 8. In other words, film of varying effective stretch ratio was produced at different TD positions. Yet the film made throughout these experiments had less than 3% gauge variation and no visual defects. This exemplifies the hidden non-uniformities this method can help detect.

References

1. A, J. Bur, M. G. Vangel and S. C. Roth, Polym. Eng. Sci., **41**, 1380 (2001).
2. A. J. Bur, S. C. Roth and C. L. Thomas, Rev. Sci. Instrum., 71, 1516 (2000).
3. A. J. Bur, R. E. Lowry, S. C. Roth and C. L. Thomas, Macromolecules, 25, 3505 (1992).
4. Identification of a commercial product is made only to facilitate experimental reproducibility and to describe adequately the experimental procedure. In no case does it imply endorsement by NIST or that it is necessarily the best product for the experiment.
5. A. Hald, "Statistical Theory with Engineering Applications", J. Wiley & Sons (1952), p.118.

Keywords: polymer films processing, biaxial orientation, polypropylene, fluorescence anisotropy

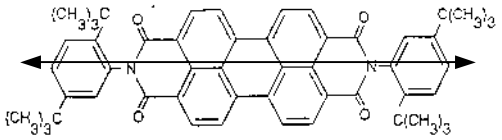

Figure 1. Molecular structure of BTBP.

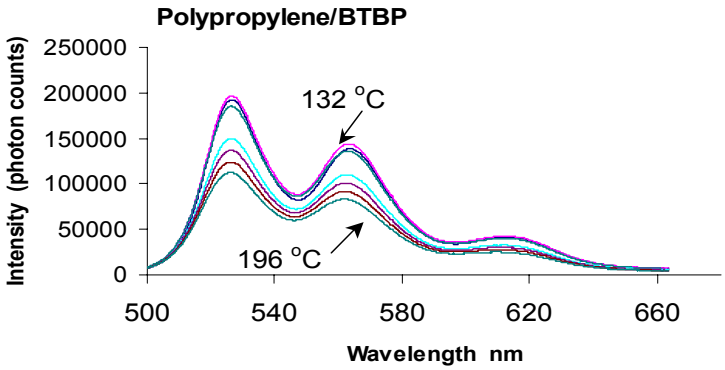

Figure 2. Spectra of BTBP doped into polypropylene at 132 °C, 143 °C. 154 °C, 165 °C, 175 °C, 185 °C and 196 °C.

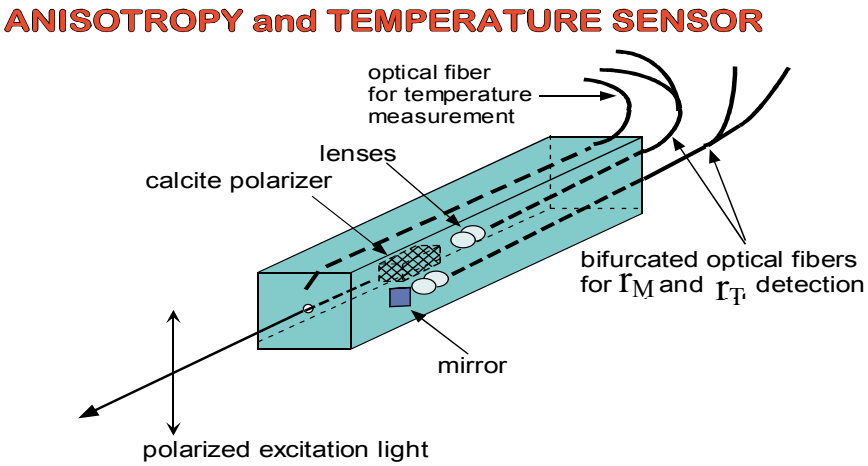

Figure 3.

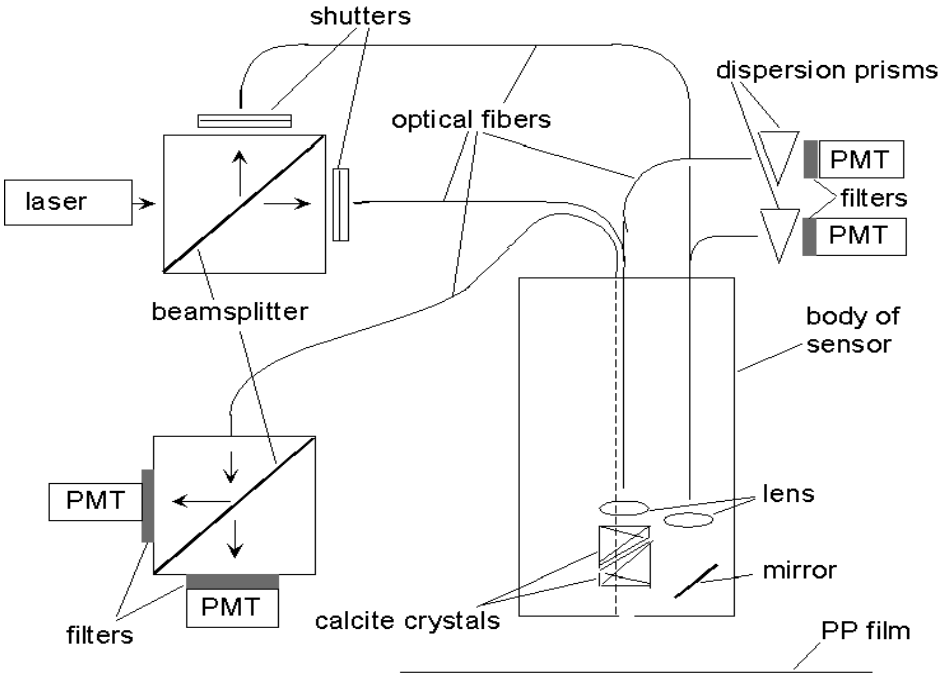

Figure 4. The experimental setup for fluorescence temperature and anisotropy measurements

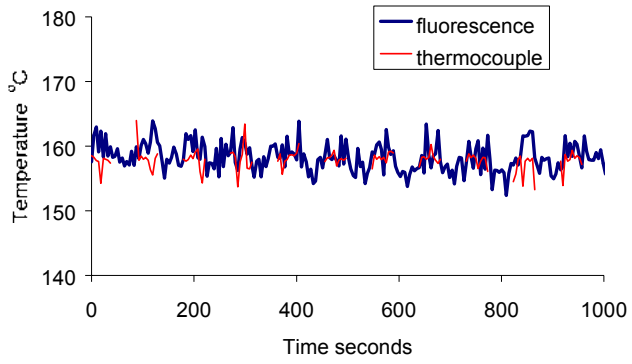

Fig. 5: Real-time fluorescence and thermocouple temperature measurements

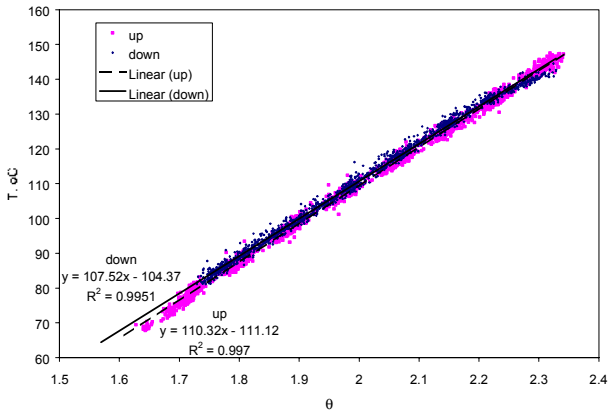

Fig. 6: Calibration of fluorescence temperature in oven

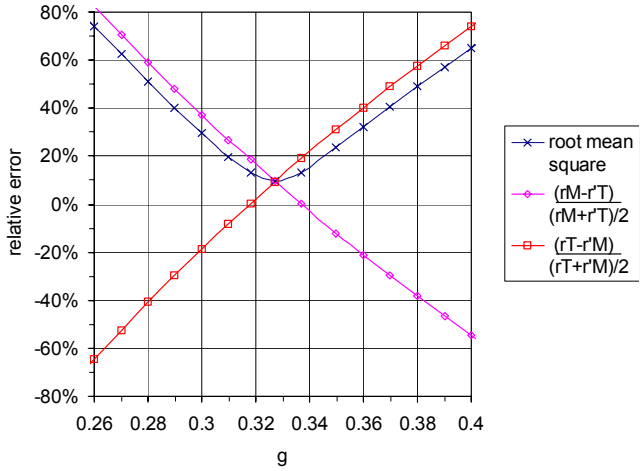

Fig. 7: g-factor calibration

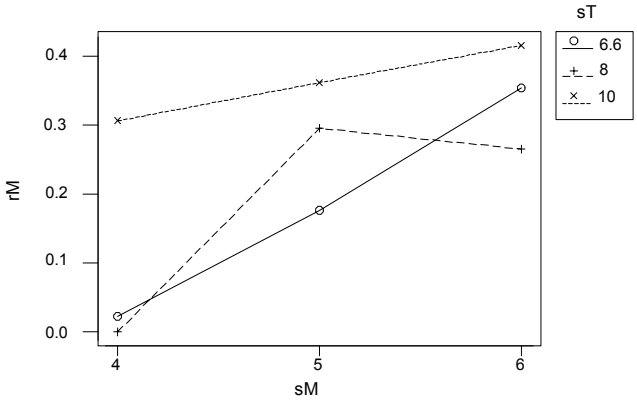

Fig. 8: Anisotropy r_M as a function of MD stretch ratio at various TD stretch ratios

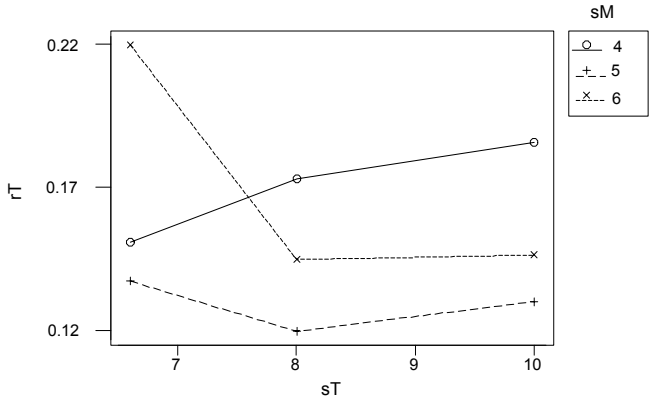

Fig. 9: Anisotropy r_T as a function of TD stretch ratio at various MD stretch ratios

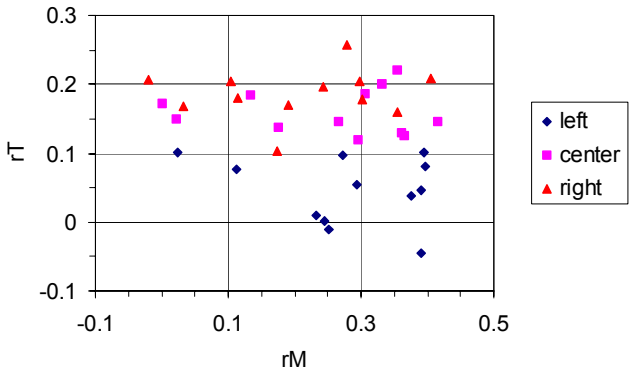

Fig. 10: r_T vs. r_M for all nine stretch ratio experiments and all three TD positions